7th International Conference on the Durability of Concrete Structures
20-22 May 2021
University of Jinan, Jinan, Shandong, China

Application of Acoustic Emission Technology in Monitoring Corrosion Cracks of Reinforced Concrete

Zeng Zhen, Xu Gang, Wang Qing, Yang Ze Wen, and Zhang Rui
College of Civil Engineering & Architecture, China Three Gorges University

ABSTRACT

Acoustic emission (AE) technology is used to monitor the whole process of reinforced concrete corrosion cracking, and the accuracy of AE technology to distinguish the location and type of cracks in concrete rust expanding and cracking are studied and verified. The results show that the Geiger algorithm positioning results correlate well with the actual fracture location; moment tensor inversion can accurately identify crack sources such as shear source, tensile source, and mixed source; it is feasible to use acoustic emission technology to locate and identify cracks.

1. INTRODUCTION

Reinforced concrete materials are widely used in various building structures due to their advantages of high strength, durability, modulus, fire resistance, and good seismic performance, but they also have the disadvantage of durability.

The external or internal environment on concrete structure leads to the development of pores, microcracks, and cracks, which will reduce the durability of the concrete structure. Therefore, a timely understanding of the development of internal microcracks in the service process of reinforced concrete structures provides an essential basis for assessing the health of concrete structures. Acoustic emission is a new type of dynamic non-destructive testing method to judge the degree of internal damage according to the stress wave emitted by the internal structure.

Acoustic emission can locate the corrosion area, reflect the corrosion state of concrete, and detect the corrosion more quickly. However, acoustic emission has many applications in mechanical testing of corroded reinforced concrete specimens [1-3], with less discussion on monitoring the process of corrosion expansion [4]. At present, acoustic emission is mainly analyzed by AE parameters, which can only get the development trend and state of concrete internal fracture, but cannot get the location of the fracturing source, and cannot bring convenience for flaw detection, monitoring, and forecasting and corresponding disposal. Therefore, using a more effective signal analysis method has important theoretical significance and practical application value for improving the state evaluation of concrete structures.

Therefore, in this paper, the anodic accelerated corrosion method is used to simulate the process of corrosion cracking, and the acoustic emission and strain monitoring are carried out throughout the whole process. The location method and the moment tensor inversion method are used to analyze and study the location and type of the crack source.

2. Moment Tensor Inversion Theory Based on AE Signal

2.1 Acoustic emission source location

The accuracy of acoustic emission localization is related to many factors, such as the setting of acoustic emission instrument parameters, the selection of wave velocity, the spatial position of the sensor, and the environmental impact. Acoustic emission detection objects are different, and localization methods are also different [5]. At present,

the application and research of source localization methods based on acoustic emission mainly focus on regional localization, time-difference localization, and spatial localization [6]; among them, the location method is based on signal TDOA. (time difference of arrival)is widely used [7]. This method has different models in different situations, such as linear location, plane location, location at the spherical surface, spatial location, etc.

The Time-difference localization method [8] mainly calculates the position of the acoustic emission source based on the time difference between the acoustic emission source being received by different sensors. Adjacent sensors S_i and S_{i+1}, the time-difference of receiving the same acoustic emission signal source is $\Delta t = T_{i+1} - T_i$ （ T_i and T_{i+1} are when acoustic emission signals arrive at S_i and S_{i+1} sensors, respectively）. Then the distance between the acoustic emission source and the sensor S_i is:

$$d = \frac{1}{2}\left(D - \Delta t v\right) \qquad (1)$$

Therefore, for the acoustic emission source in space (x, y, z), the relationship between the acoustic emission source and the location of each sensor (x_i, y_i, z_i) can be expressed as the following function (2) when the time difference t_i between the signal generated by it and the sensor is known.

$$\sqrt{(x-x_i)^2 + (y-y_i)^2 + (z-z_i)^2} = v(t_0 + t_i) \qquad (2)$$
$$i = 1, 2, \ldots n$$

Where n is the number of sensors, t_0 is the time for the signal to reach the probe closest to the acoustic emission source, and v is the wave velocity.

The current localization algorithms mainly include relative localization, least squares method [9], Geiger algorithm [10], etc. Geiger algorithm is widely used in the seismic source location. The principle is to assume that an initial acoustic emission source is close to the actual acoustic emission source (x, y, z) by iteratively modifying the source, that is, the time residual is the smallest, and the corresponding objective function is :

$$\phi(x, y, z, t_0) = \sum_{i=1}^{n} r_i^2 \qquad (3)$$
$$i = 1, 2, \ldots n$$

Where r_i is the time residual, $r_i = t_i + t_0 - T_{i0}(x, y, z)$, and $T_{i0}(x, y, z)$ is the assumed acoustic emission source to each probe, as shown in the following function（4）：

$$T_{i0}(x, y, z) = \frac{\sqrt{(x-x_i)^2 + (y-y_i)^2 + (z-z_i)^2}}{v} \qquad (4)$$

The iterative calculation process of the Geiger algorithm is based on the Taylor expansion $T_{i0}(x, y, z)$, which omits the high-order component, converts the nonlinear term into a linear term, and then continuously modifies the initial value for an iteration. The final positioning result is obtained when the time residual meets the corresponding requirements.

2.2 Moment tensor inversion

Due to the close relationship between acoustic emission, microseismic, and earthquake, many theories of acoustic emission have evolved from earlier seismological theories. Gilbert [11] proposed the concept of moment tensor in 1971, which is defined as the first-order moment of equivalent volume force acting on a point. The moment tensor contains the radiation energy information of the earthquake and the nodal plane directions of the shear fracture components and the isotropic components. The moment tensor is used to represent the source without any assumption of the source mechanism in advance, and the far-field displacement is expressed as a linear relationship with the moment tensor [12].

The theoretical basis of moment tensor inversion in seismology is elastic wave theory, and acoustic emission also belongs to the elastic wave range, so moment tensor theory can also be used in acoustic emission research. Ohtsu [13] introduced the simplified Green's function moment tensor analysis (SIGMA) into acoustic emission data analysis and

used the peak value of P wave (primary wave, which are the first waves from an earthquake to arrive at a seismograph). Initial dynamic displacement in the waveform to inverse the moment tensor. The acoustic emission sources of cracks were divided into shear, tensile, and mixed cracks. The moment tensor inversion mechanism [14] is shown in Figure 1.

Referring to the method of Ohtsu [13], for homogeneous and isotropic materials, the P-wave in the whole space Green's function is selected, only the P-wave in the initial wave of acoustic emission is considered, and the far-field approximation condition is satisfied (source distance R is much larger than source region radius L; acoustic emission signal wavelength is greater than L), and only the initial amplitude of P wave is involved. For the signals monitored by acoustic emission technology, the initial amplitude A(*x*) of the P wave is expressed as the following function (5) :

$$A(x) = C_s \, Re\, f(\bar{t},\bar{r}) \frac{\gamma_p m_{pq} \gamma_q}{R} \qquad (5)$$

Function (5) can be further expanded to obtain:

$$A(x) = C_s \, Re\, f(\bar{t},\bar{r})(r_1, r_2, r_3) \begin{pmatrix} m_{11} & m_{12} & m_{13} \\ m_{12} & m_{22} & m_{23} \\ m_{13} & m_{23} & m_{33} \end{pmatrix} \begin{pmatrix} r_1 \\ r_2 \\ r_3 \end{pmatrix} \qquad (6)$$

Where: C_s is the physical coefficient of sensor sensitivity, *R* is the distance from the crack occurrence point *y* to the detection point *x*, that is, the distance from the AE source to the acoustic emission sensor(see Figure 2); r_1, r_2, and r_3 are the direction cosine of *R* on each coordinate axis； $Re\, f(\bar{t},\bar{r})$ is the reflection coefficient of the surface where the sensor is installed; $\bar{t}$ is the direction of the sensitivity of the acoustic emission sensor.

For $Re\, f(\bar{t},\bar{r})$, function (7) can be used to solve :

$$Re\, f(\bar{t},\bar{r}) = \frac{2k^2 a(k^2 - 2[1-a^2])}{(k^2 - 2[1-a^2])^2 + 4a[1-a^2]\sqrt{k^2 - 1 + a^2}} \qquad (7)$$

Where: $k=v_p/v_s$., a is the inner product of vector $\bar{r}$ and vector $\bar{t}$. When the signal vertically reaches the sensor surface, *a*=1, $Re\, f(\bar{t},\bar{r}) = 2$。

The moment tensor contains nine values, but it is a second-order symmetric vector, so it is equivalent to only six independent unknowns. If there are more than six sensors on the specimen, according to the initial amplitude of the initial acoustic emission received by each sensor, the equation group becomes an overdetermined equation group. Because the equations are linear and independent of time, the solution of the moment tensor can be obtained by function (6). After obtaining the moment tensor of the fracturing source, the fracture type can be associated with the moment tensor through the equivalent model. By decomposing the moment tensor and comparing it with the tension source's equal effect model and the shear source's equal effect model, the type of fracture source can be determined.

According to Ohtsu's s SIGMA analysis method [15], three eigenvalues of the moment tensor are obtained: the maximum eigenvalue e_1, the intermediate eigenvalue e_2, and the minimum eigenvalue e_3. Because the tension-type and shear-type of the crack do not both represent that the crack is a pure tensile failure or pure shear failure, there may be two kinds of failure in the crack, but the proportion of the two is different, that is, the contribution of the two to the failure of the crack is different. At this time, the significant failure type of the crack can be regarded as the pure failure type. Because the inversion in this paper adopts relative inversion, it is not necessary to solve the specific value of *X*, *Y*, *Z*, according to the function (8), the relative ratio of X, Y, Z can be :

$$\begin{aligned} \frac{e_1}{e_1} &= X + Y + Z \\ \frac{e_2}{e_1} &= 0 - \frac{Y}{2} + Z \\ \frac{e_3}{e_1} &= -X - \frac{Y}{2} + Z \end{aligned} \qquad (8)$$

In function (8), *X* can represent the shear ratio, that is, the contribution of shear cracks in the fracture model; *Y* can represent tension deviation ratio, *Z* can represent tension isotropic ratio, *Y*+*Z* can be regarded as the contribution value of tension mode in fracture model. Therefore, if it is a pure shear crack, X=100%, Y=Z=0; on the contrary, if it is a pure tension crack, then X=0, Y+Z=100%. Based on a large number of test results [16], fracture types can be classified according to the value of shear ratio X:

$$\begin{cases} X > 60\%\left(Y+Z<40\%\right), \textit{Shear crack} \\ 40\% \le X \le 60\%, \textit{Mixed crack} \\ X < 40\%\left(Y+Z>60\%\right), \textit{Tensile crack} \end{cases} \quad (9)$$

After the eigenvalues of the moment tensor are obtained, the corresponding eigenvectors can be further solved. The feature vector $\vec{e_1}$, $\vec{e_2}$, $\vec{e_3}$, which can be expressed by the crack motion vector $\vec{l}$ and the crack surface normal vector $\vec{n}$, and the relational expression is shown in function (10) :

$$\begin{aligned} \vec{e_1} &= \vec{l} + \vec{n} \\ \vec{e_2} &= \vec{l} \times \vec{n} \\ \vec{e_3} &= \vec{l} - \vec{n} \end{aligned} \quad (10)$$

where× represents the vector product. If the shear ratio X is used to determine the tensile crack, the motion vector $\vec{l}$ and the normal vector $\vec{n}$ are parallel, and the direction of $\vec{e_1}$ is the direction of $\vec{l}$ or $\vec{n}$, which is the direction of cracking; If the shear ratio X is determined as shear crack, the motion vector $\vec{l}$ and normal vector $\vec{n}$ are vertical, and the direction of $\vec{l}$ is the cracking direction of the crack; Both $\vec{l}$ and $\vec{n}$ can be obtained from $\left(\vec{e_1}+\vec{e_3}\right)$ and $\left(\vec{e_1}-\vec{e_3}\right)$ Application of acoustic emission in crack monitoring of reinforced concrete.

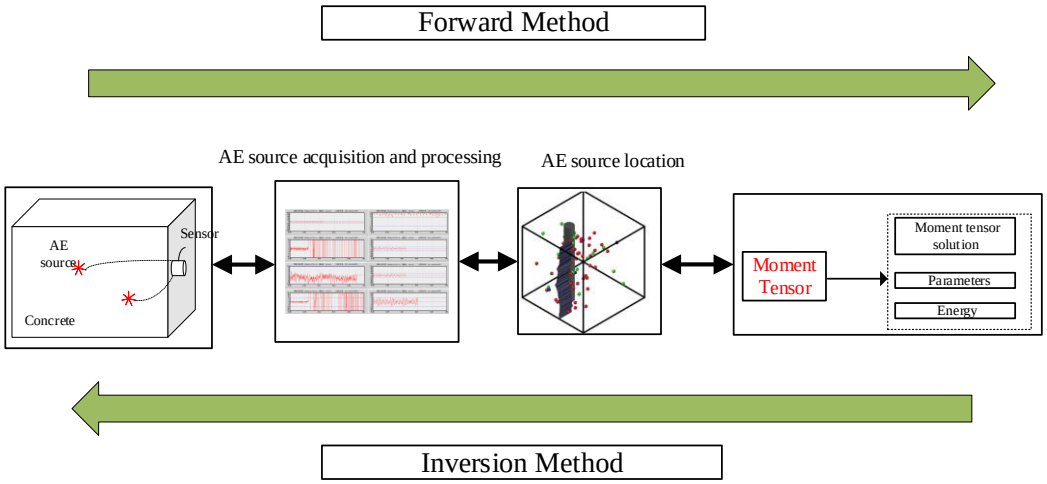

Figure 1. Schematic diagram of moment tensor inversion mechanism

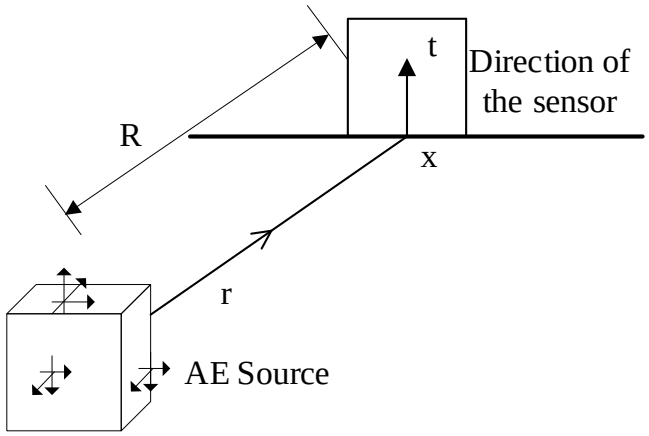

Figure 2. Diagram of geometrical relationship between AE source and sensor

3. Corrosion-induced cracking test

3.1. Setup of the experiment

Specimens 120mm long were cut from 20mm-diameter HPB300 steel robs. The test area is a section with a length of 100mm. That is, the test section is buried in the concrete.

The size of the concrete specimen is 150mm × 150mm × 150mm, and the thickness of the protective layer is 30mm. The positions of steel bars and strain gauges are shown in Figure 3. Paste strain gauges on the four sides of a square with a side length of 50mm centered on the steel bar, then wires are welded, and epoxy resin is poured on it to prevent the rusty water from overflowing over the surface of the strain gauge and causing it to fail(see Figure 4). For strain monitoring, the specimen began to collect three days before the beginning of the power， as a blank collection before power, the instrument is a UT7100 acquisition instrument, connected by a 1/4 bridge, with the same size strain gauge attached to the accompanying specimen as a common compensation, and data is collected every ten minutes.

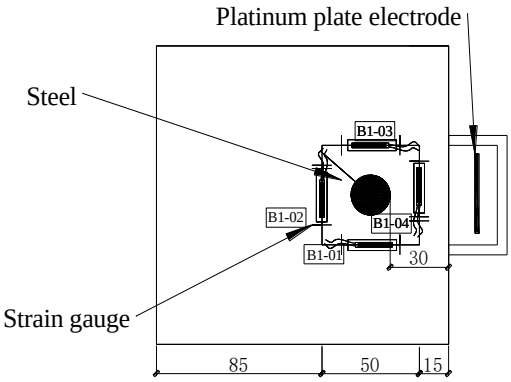

Figure 3. Prone view of the specimen

The current density on the surface of the steel bar is 600$\mu A/cm^2$, and the total current is 37.68mA. Before accelerated corrosion, a flume is installed on the side of the specimen near the reinforcement. The size and location of the flume are shown in Figure 5(a). After installation, 3.5 % NaCl solution is filled into the flume and soaked for three days to reduce the resistance of the concrete protective layer. Three days later, stainless steel sheets were placed in the tank, connected with the negative electrode of the constant current power supply as the cathode, and the steel bars were connected with the positive electrode of the power supply as the anode, as shown in Figure 5(b).

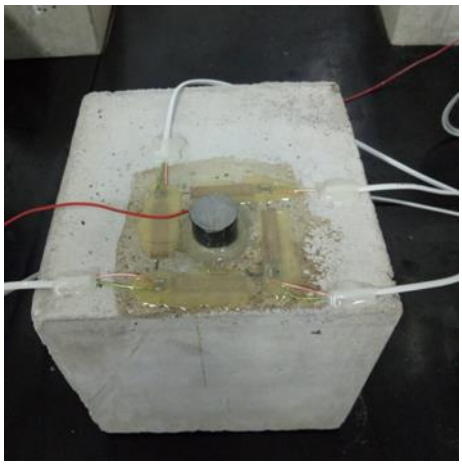

Figure 4. Strain gauge arrangement

In order to locate the corrosion process of steel bar in three-dimensional acoustic emission, the whole process of steel bar corrosion was monitored by 8-channel SEAU2S digital acoustic emission system. The selected preamplifier gain is 60dB, and the acoustic emission probe is Shenghua SR150N resonant narrow-band probe.

To make each channel have a similar sensitivity to the stress wave generated by the crack source, parameter settings, gain sizes, and AE sensors for each channel are consistent. Six sensors are uniformly distributed on concrete specimens' top, left, and right surfaces, as shown in Figure 6 (a). The coupling between the sensor and concrete is fixed by hot melt adhesive (see Figure 6(b)), which can keep the probe close to the specimen, but its acoustic impedance is more significant than that of common coupling agents such as Vaseline.

In the acoustic emission localization, the wave velocity is set to be known and constant. In order to obtain accurate wave velocity, this paper uses NM-4A non-metallic ultrasonic testing analyzer to test the same batch of mortar cube specimens. It uses the measured P wave velocity to replace the wave velocity in the acoustic emission positioning calculation.

Among them, the ultrasonic spectrum of acoustic emission shows that its peak frequency is 43 kHz,

which is close to the signal frequency band obtained by our previous experimental monitoring [17] and can replace the actual acoustic emission wave velocity. which is close to the signal frequency band obtained by monitoring and can replace the actual AE wave velocity. Monitoring results of Corrosion-induced cracking.

The moment tensor inversion analysis is based on the moment tensor inversion of the initial displacement peak of the P wave in the waveform to obtain the moment tensor matrix. Then, through the classification of the matrix, the acoustic emission sources of cracks are divided into shear cracks, tensile cracks, and mixed cracks. According to the above analysis method, the programming calculation is carried out to obtain the positioning results and pick up the initial dynamic position and initial arrival time of p wave, and finally, the type of corrosion crack is obtained.

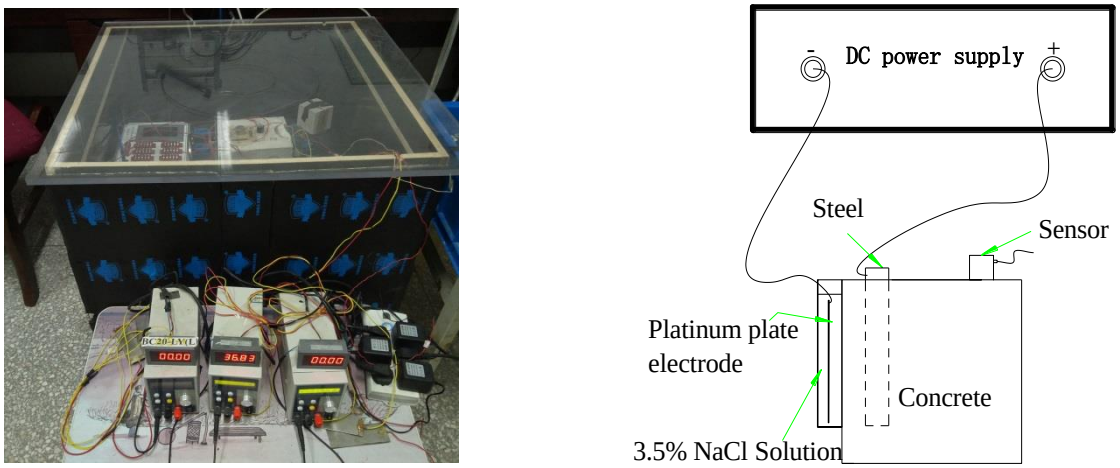

（a）Test monitoring process　　（b）Electric accelerated corrosion

Figure 5. Monitoring of Electrical Accelerated Corrosion Test

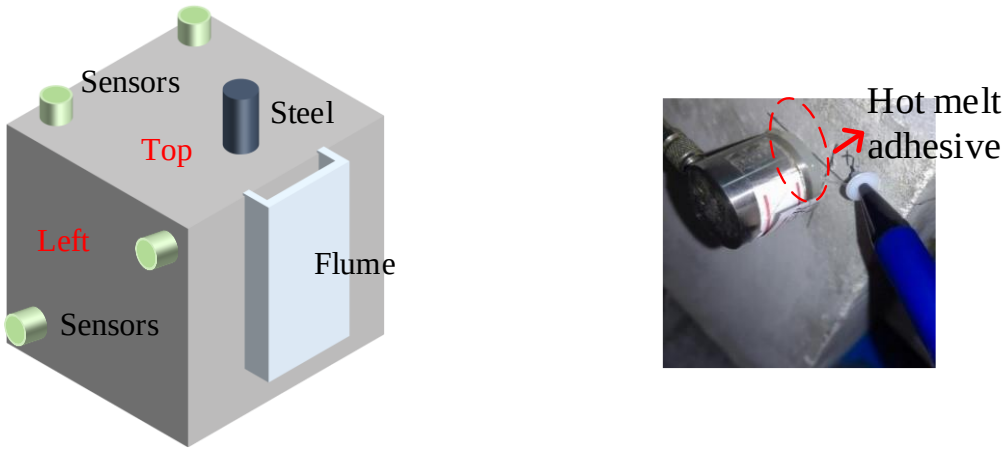

（a）Sensors layout diagram　　（b）Sensor coupling detection

Figure 6. The layout diagram of acoustic emission sensor

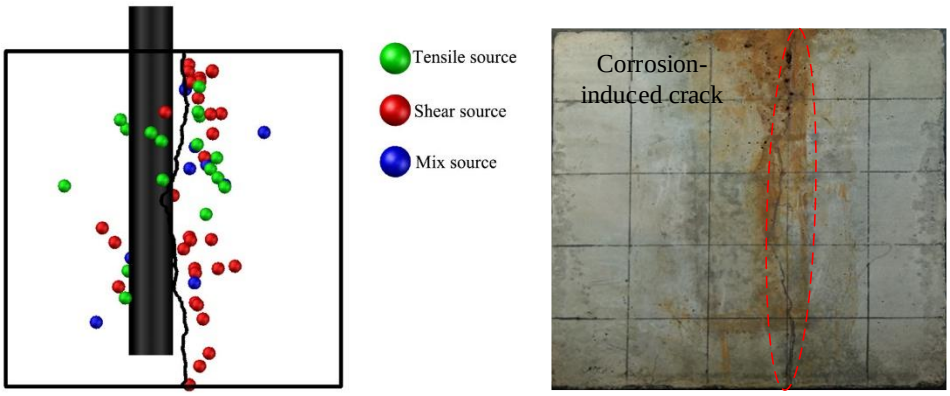

（a）Moment tensor inversion results　　（b）Test result

Figure 7. Distribution map of rust expansion cracks

In the moment tensor inversion analysis, for each analysis of the AE event, six channels are needed to capture the signal of the same event acoustic emission source at the same time, and the algorithm can successfully and effectively identify the initial movement position and the first arrival time of the p-wave.

The result of the analysis is shown in Figure 7. From the results, according to the Geiger localization algorithm, the calculation results correspond to the location of corrosion-induced cracking in the test. According to the previous research of the research group [18], in the environment of accelerated corrosion by electricity, there is an oxygen evolution reaction, which will produce signal sources such as bubble desorption and rupture. Therefore, the location point outside the fracture area may be corresponding to the oxygen generated by the oxygen evolution reaction overflowing outward or the internal damage that cannot be observed.

4. Conclusion

（1）The time difference between the first arrival of the P wave is used to calculate the time difference, and then the Geiger algorithm is used for the positioning calculation, and the result can better reflect the position of the crack.

（2）Based on the moment tensor theory, the corrosion-induced cracking source can be divided into the shear, tensile, and mixed sources by analyzing the experimental data. Its accuracy needs further verification.

REFERENCES

1. D. Yoon, W.J. Weiss, S.P. Shah. 2000. Assessing Damage in Corroded Reinforced Concrete Using Acoustic Emission. J ENG MECH. 126, 273-283.
2. A. Abouhussien, A. Hassan. 2016. Application of Acoustic Emission Monitoring for Assessment of Bond Performance of Corroded Reinforced Concrete Beams. Structural Health Monitoring. 16.
3. A. Zaki, H.K. Chai, A. Behnia, D.G. Aggelis, J.Y. Tan, Z. Ibrahim. 2017. Monitoring Fracture of Steel Corroded Reinforced Concrete Members Under Flexure by Acoustic Emission Technique. CONSTR BUILD MATER. 136, 609-618.
4. P. Kot, M. Muradov, M. Gkantou, G.S. Kamaris, K. Hashim, D. Yeboah. 2021. Recent Advancements in Non-Destructive Testing Techniques for Structural Health Monitoring. A.P.P.L. SCI-BASEL. 11.
5. M. Ge. 1997. Comparison of Least Squares and Absolute Value Methods in Ae/M.S. Source Location: A Case Study. International Journal of Rock Mechanics & Mining Sciences. 34, 637-646.
6. G. McLaskey, S. Glaser, C. Grosse. 2010. Beamforming Array Techniques for Acoustic Emission Monitoring of Large Concrete Structures. J SOUND VIB. 329, 2384-2394.
7. P. Kundu, K. N K, A.K. Sinha. 2009. A Non-Iterative Partial Discharge Source Location Method for Transformers Employing Acoustic Emission Techniques. Applied Acoustics - APPL ACOUST. 70, 1378-1383.

8. G.T. Shen, R.S. Geng, S.F. Liu. 2002. Acoustic Emission Source Location. Nonde Structive Testing, 24-27. (in Chinese)
9. Y.M. Kang, J.P. Liu, H.B. Li, C.H. Wei. 2010. An AE Source Location Combination Algorithm Based on Least Square Method. Journal of Northeastern University(Natural Science). 31, 1648-1651. (in Chinese)
10. J. Liu, G. Jian. 2012. Hypocenter Location by Using Combined Method of Inglada and Geiger Algorithms. Journal of Institute of Disaster Prevention, 57-62.
11. F. Gilbert. 1971. Excitation of the Normal Modes of the Earth by Earthquake Sources. GEOPHYS J INT. 22, 223-226.
12. M.C.A.P. Kurose. 2007. FLAC/PFC Coupled Numerical Simulation of AE in Large-Scale Underground Excavations. INT J ROCK MECH MIN.
13. M. Ohtsu. 1991. Simplified Moment Tensor Analysis and Unified Decomposition of Acoustic Emission Source: Application to in Situ Hydrofracturing Test. Journal of Geophysical Research Atmospheres. 96.
14. K. Aki, P. 2002. Richards. Quantitative Seismology.
15. M. Ohtsu. 1991. Simplified Moment Tensor Analysis and Unified Decomposition of Acoustic Emission Source: Application to in Situ Hydrofracturing Test. JOURNAL OF GEOPHYSICAL RESEARCH.
16. M. Ohtsu, M. Shigeishi, H. Iwase, W. Koyanagit. 2015. Determination of Crack Location, Type, and Orientation Ina Concrete Structures by Acoustic Emission. Magnetism & Magnetic Materials —: Nineteenth Conference.
17. X.U. Gang, Z. Zeng, R. Zhang, Y. Peng, Z. Yang. 2019. Characteristics of Acoustic Emission Signals from Initial Corrosion of Steel Bar in Cement-Based Materials. Journal of Building Materials. 22, 385-393. (in Chinese)
18. Z. Rui. 2017. The Acoustic Emission Monitoring of Concrete Members Corrosion Damage and Analysis of the Signal Source [Yichang: China Three Gorges University; (in Chinese)